Electronic States and Spectroscopic Properties of SiTe and SiTe+

ARTICLE *in* THE JOURNAL OF PHYSICAL CHEMISTRY A · DECEMBER 2006

Impact Factor: 2.69 · DOI: 10.1021/jp062610c · Source: PubMed

4 AUTHORS, INCLUDING:

Surya Chattopadhyaya
Tripura University
16 PUBLICATIONS **61** CITATIONS
SEE PROFILE

Anup Pramanik
Visva Bharati University
27 PUBLICATIONS **98** CITATIONS
SEE PROFILE

Electronic States and Spectroscopic Properties of SiTe and $SiTe^+$

Surya Chattopadhyaya,[†] Anup Pramanik, Amartya Banerjee, and Kalyan Kumar Das*

Department of Chemistry, Physical Chemistry Section, Jadavpur University, Kolkata 700 032, India

Received: April 28, 2006; In Final Form: August 23, 2006

Ab initio based configuration interaction calculations have been carried out to study the low-lying electronic states and spectroscopic properties of the heaviest nonradioactive silicon chalcogenide molecule and its monopositive ion. Spectroscopic constants and potential energy curves of states of both SiTe and $SiTe^+$ within 5 eV are reported. The calculated dissociation energies of SiTe and $SiTe^+$ are 4.41 and 3.52 eV, respectively. Effects of the spin−orbit coupling on the electronic spectrum of both the species are studied in detail. The spin−orbit splitting between the two components of the ground state of $SiTe^+$ is estimated to be 1880 cm^{-1}. Transitions such as 0^+(II)-$X^1\Sigma^+_{0^+}$, 0^+(III)-$X^1\Sigma^+_{0^+}$, E $^1\Sigma^+_{0^+}$-$X^1\Sigma^+_{0^+}$, and $A^1\Pi_1$-$X^1\Sigma^+_{0^+}$ are predicted to be strong in SiTe. The radiative lifetime of the $A^1\Pi$ state is less than a microsecond. The $X_2{}^2\Pi_{1/2}$-$X_1{}^2\Pi_{3/2}$ transition in $SiTe^+$ is allowed due to spin−orbit mixing. However, it is weak in intensity with a partial lifetime for the X_2 state of about 108 ms. The electric dipole moments of both SiTe and $SiTe^+$ in their low-lying states are calculated. The vertical ionization energies for the ionization of the ground-state SiTe to different ionic states are also reported.

I. Introduction

Over the last few decades, there have been a number of experimental studies on silicon chalcogenide molecules.[1−10] Of all the chalcogenides, the lightest species SiO/SiO^+ have been studied the most. These molecules play key roles in interstellar and circumstellar chemistry. However, the number of investigations is considerably fewer for the heavier species. Barrow and co-workers[1] have made pioneering work in this regard. The ultraviolet D−X systems of the red-degraded bands of SiSe and SiTe have been developed in high-temperature discharge through silica tubes which contain aluminum selenide and a mixture of aluminum and tellurium powders, respectively.[2,3] The vibrational analyses of these bands have also been carried out. For SiTe, about 25 bands have been measured between 3290 and 3900 Å with 0−0 band at 3496.6 Å. However, the 0−0 band is not found to be very intense. Another ultraviolet E−X band system has been observed[4] for each of the SiS, SiSe, and SiTe molecules in absorption at high temperature (800−1000 °C). The D−X systems, which are known in emission, have also been photographed in absorption. The vibrational analyses have provided vibrational constants of X, D, and E states. Keeping an analogy with SiO and SiS, the lowest excited state (D) of SiTe has been presumed to be $^1\Pi$. The state has been renamed as $A^1\Pi$ for the lighter molecules. However, these studies have wrongly suggested that the E state of SiTe is of the $^3\Sigma^+$ symmetry. Thermodynamic studies[5,6] of SiTe have reported an average dissociation energy (D^0_0) of 4.64 eV. The high-resolution studies of either $A^1\Pi$-$X\ ^1\Sigma^+$ or E $^1\Sigma^+$-$X^1\Sigma^+$ have not been carried out for SiTe, while these are known for SiSe.[7] A high-temperature photoelectron spectroscopy[8] of SiS in the ground state has been carried out in order to obtain the spectral feature of the ground and excited states of SiS^+. A set of weak bands arising from the spin-forbidden transition $a^3\Pi$-$X^1\Sigma^+$ has been studied by Lebreton et al.[9] in the region of 3900−4300 Å from the emission spectrum of SiSe in the low current discharge. Bosser et al.[10] have carried out the high-resolution rotational analyses of $D^1\Pi$-$X^1\Sigma^+$ and $a^3\Pi_1$-$X^1\Sigma^+$ transitions of SiSe. Recently,[11] ab initio based configuration interaction (CI) studies of $SiSe^+$ have been performed, but no experimental or theoretical studies have been reported for the $SiTe^+$ ion so far.

In this article, we report the electronic states and spectroscopic properties of both SiTe and $SiTe^+$ obtained from the multireference singles and doubles CI (MRDCI) calculations with relativistic effects and spin−orbit coupling taken in consideration. Since the tellurium atom is quite heavy, the spin−orbit coupling plays an important role in characterizing the electronic spectra of these species. Potential energy curves of the ground and low-lying states of SiTe and $SiTe^+$ have been constructed with and without spin−orbit coupling. Spectroscopic constants are estimated and compared with the existing data. Transition dipole moments of some selected transitions are computed. Electric dipole moments and radiative lifetimes of the excited states of both SiTe and $SiTe^+$ are also the subject of the present study.

II. Computational Details

The $1s^22s^22p^6$ core electrons of Si have been substituted by the relativistically corrected effective core potentials (RECP) of Pacios and Christiansen,[12] while the $3s^23p^2$ valence electrons are considered for the CI calculations. The tellurium atom is quite heavy, and 36 core electrons are described by the semicore type RECP of LaJohn et al.[13] Therefore, the valence space of Te consists of $4d^{10}5s^25p^4$ electrons for CI calculations. Therefore, for the SiTe molecule, the total number of active electrons is 20, while for its monopositive ion it is 19. The (4s4p) primitive Gaussian basis sets of Si have been taken from Pacios and Christiansen.[12] The additional polarization and diffuse functions are taken from Matos et al.[14] The final AO basis of Si used in the calculation of both the species is (7s6p5d2f)/[7s6p4d1f]. The exponents and contraction coefficients of these

* Corresponding author e-mail: kkdas@chemistry.jdvu.ac.in and das_kalyank@yahoo.com.

[†] Present address: Department of Physics, Ramkrishna Mahavidyalaya, Kailashahar, Tripura 799277, India.

10.1021/jp062610c CCC: $33.50
Published on Web 10/17/2006

augmented functions are given elsewhere.[14] For the tellurium atom, the (3s3p4d) Gaussian basis sets of LaJohn et al.[13] have been augmented with one set of f functions with an exponent of 2.5 a_0^{-2} taken from Setzer et al.[15] Therefore, the final AO basis function of Te is (3s3p4d1f).

Throughout the calculations, SiTe and $SiTe^+$ are aligned along the *z* axis with Si at the origin. The calculations have been carried out in the C_{2v} subgroup of the full symmetry. The SCF calculations have been carried out for the $(\sigma^2\pi^4)$ $^1\Sigma^+$ state of SiTe and $(\sigma\pi^4)$ $^2\Sigma^+$ state of $SiTe^+$ at each internuclear distance. Since 10 inner d electrons of the Te atom do not participate in the chemical bonding, we have kept them frozen in the configuration space. The number of active electrons reduces to 10 and 9 for SiTe and $SiTe^+$, respectively. In addition, we have discarded some of the very high energy MOs. The total number of SCF-MOs, which are used as one-electron basis functions for the CI calculations, becomes 90. The MRDCI methodology of Buenker and co-workers[16−22] has been used throughout the calculations. The method uses perturbative correction and energy extrapolation techniques. A set of reference configurations is chosen for each of the four irreducible representations of C_{2v} for a given spin and spatial symmetry. Nine lowest roots are calculated for singlet and triplet spin multiplicities, while five roots are computed for quintets of SiTe. For the ion, six and four lowest roots are optimized for doublets and quartets, respectively. The single and double excitations are carried out from the selected set of reference configurations. A configuration-selection threshold of 1.0 μhartree has been chosen to keep total selected configurations below 200 000. We have used Table Direct-CI version[23] of the MRDCI code throughout. The sum of squares of coefficients of the reference configurations for each root remains above 0.9.

To study the effects of the spin−orbit coupling, we have employed those spin−orbit operators which are compatible with the RECPs of Si and Te atoms. The spin−orbit operators of Si have been taken from Pacios and Christiansen,[12] while those reported by LaJohn et al.[13] have been employed for Te. In the C_{2v} double group, the Ω states of SiTe belong to A_1, A_2, and B_1/B_2, while for $SiTe^+$, these correspond to E_1 and E_2 representations. The two-step variational method[13−16] has been employed for the spin−orbit calculations, the details of which are discussed elsewhere.[24]

Spectroscopic constants of the low-lying states of SiTe and $SiTe^+$ have been estimated, both including and omitting the spin−orbit interaction, by fitting the potential energy curves. The vibrational energies and wave functions are then obtained from the numerical solutions of the one-dimensional nuclear Schrödinger equations. Einstein spontaneous emission coefficients, transition probabilities, and radiative lifetimes of excited states are calculated.

III. Results and Discussion

Potential Energy Curves and Spectroscopic Constants of Λ-S States. There are 18 Λ-S states of SiTe correlating with the lowest dissociation limit, $Si(3p^2;\ ^3P_g)+Te(5p^4;\ ^3P_g)$. These electronic states have singlet, triplet, and quintet spin multiplicities. The second dissociation limit, $Si(3p^2;\ ^1D_g)+Te(5p^4;\ ^3P_g)$, generates nine states of triplet spin multiplicity. The relative energy of the second dissociation limit computed from the calculations of SiTe at a very large bond distance agrees well with the data obtained from the atomic energy table.[25] The lowest dissociation limit, $Si^+(3p;\ ^2P_u)+Te(5p^4;\ ^3P_g)$, correlates with 12 Λ-S doublets and quartets of the $SiTe^+$ ion, while nine doublets dissociate into the second asymptote $Si^+(3p;\ ^2P_u)+Te(5p^4;\ ^1D_g)$. The calculated relative energy of the second dissociation limit has been compared with the *J*-averaged observed value, and a discrepancy of about 600 cm^{-1} is noted.

TABLE 1: Spectroscopic Constants of the Λ-S States of SiTe

	T_e/cm^{-1}		r_e/Å		ω_e/cm^{-1}	
state	calc	expt	calc	expt	calc	expt
$X^1\Sigma^+$	0		2.30		479	481.2[a]
$a^3\Sigma^+$	16 667		2.53		349	
$^3\Delta$	20 135		2.55		330	
$^3\Sigma^-$	22 200		2.59		315	
$^1\Sigma^-$	22 237		2.59		305	
$^1\Delta$	22 436		2.60		306	
$b^3\Pi$	22 687		2.38		377	
$A^1\Pi$	29 072	28 661.8[a]	2.45		331	338.6[a]
$E^1\Sigma^+$	32 902	33 991[a]	2.70		259	242[a]
$^5\Sigma^+$	32 991		2.91		227	
$^5\Pi$	33 953		2.72		194	
$2^3\Pi$	38 862		2.89		237	

[a] Reference 4.

A. SiTe. The computed potential energy curves of all the singlet, triplet, and quintet states of SiTe correlating with the lowest dissociation limit are shown in Figure 1a−c. There are as many as 12 bound states, while the remaining states are either repulsive or predissociative. Spectroscopic constants of these bound states of SiTe are tabulated in Table 1. The ground state ($X^1\Sigma^+$) of SiTe has an equilibrium bond length of 2.30 Å with $\omega_e = 479$ cm^{-1}. The vibrational analysis of the UV band[4] has determined a value of 481.2 cm^{-1} for ω_e of the ground state in excellent agreement with the computed value. The observed[26] ground-state dissociation energy (D_0^0) of SiTe also agrees well with the calculated value of 4.65 eV. Earlier calculations[27−29] of isovalent species such as SiO, SiS, and SiSe at the same level of CI have shown that the computed D_e is underestimated by 0.3−0.6 eV because of the use of pseudopotentials, the limitation of the CI, basis set etc. The D_e value of the lighter SiSe molecule computed at the same level[29] is 5.33 eV. However, the computed D_e of SiTe shows the correct trend as $D_e(SiO) > D_e(SiS) > D_e(SiSe) > D_e$ (SiTe). The ground-state configuration of SiTe is mainly $\sigma^2\pi$,[4] where σ and π are both strongly bonding type MOs comprising the s and p_z atomic orbitals of Si and Te atoms.

The first excited state of SiTe is $a^3\Sigma^+$ which originates from a $\pi\rightarrow\pi^*$ excitation. The computed transition energy of $a^3\Sigma^+$ at equilibrium is 16 667 cm^{-1} with $r_e = 2.53$ Å and $\omega_e = 349$ cm^{-1}. The state is strongly bound with a dissociation energy of 2.58 eV. It is analogous to the $a'^3\Sigma^+$ state of the isovalent CO molecule. The $a^3\Sigma^+$-$X^1\Sigma^+$ band system of SiS has been observed in the chemiluminescent flame spectra.[30] The spin−orbit coupling in the $a^3\Sigma^+$ state of SiTe leads to the spin-forbidden transition such as $a^3\Sigma_1^+$-$X^1\Sigma_{0^+}^+$ in the range of 16 000−17 000 cm^{-1}. The $^3\Delta$ state, which is next to $a^3\Sigma^+$, also originates from the $\pi\rightarrow\pi^*$ excitation. It is strongly bound with a dissociation energy of 2.15 eV. The MRDCI estimated transition energy of this state is 20 135 cm^{-1} at $r_e = 2.55$ Å with a vibrational frequency of about 330 cm^{-1}. The $^3\Delta$ state of the isovalent SiS is, however, experimentally known.

Three nearly degenerate states, $^3\Sigma^-$, $^1\Sigma^-$, and $^1\Delta$, appear from the same $\pi\rightarrow\pi^*$ excitation that generates $a^3\Sigma^+$ and $^3\Delta$. Spectroscopic parameters of these three states are quite similar. The identical spectroscopic features of these states have also been noted for other neutral silicon chalcogenides.[27−29] Transition energies of all three states of the heaviest SiTe molecule lie in the range of 22 200−22 500 cm^{-1}. The equilibrium bond

lengths of $^3\Sigma^-$, $^1\Sigma^-$, and $^1\Delta$ are close to 2.60 Å, and their vibrational frequencies are computed to be around 310 cm^{-1}. The next important state is a strongly bound $^3\Pi$ state which is located 22 687 cm^{-1} above the ground state. The Si−Te bond in the lowest $^3\Pi$ state is shorter, and its vibrational frequency is larger than the other excited states of SiTe. The state is denoted as $b^3\Pi$ in analogy to the lighter species for which the $b^3\Pi_1$-$X\ ^1\Sigma^+$ transition has been observed.[27−29] It is also expected that such transition may also be observable in SiTe. The $b^3\Pi$ state is generated mainly due to a $\sigma\rightarrow\pi^*$ excitation.

The next important state is designated as $A^1\Pi$ which is the lowest root in this symmetry. The state is observed in the UV absorption band system,[4] and it originates from the same $\sigma\rightarrow\pi^*$ excitation as in $b^3\Pi$. The $^1\Pi$ state was originally labeled by Vago and Barrow[4] as $D^1\Pi$. However, keeping an analogy with the studies of other isomers,[22−24] we have kept the notation of this state as $A^1\Pi$. The computed transition energy of the A−X transition is about 29 072 cm^{-1}, while the vibrational analysis of the band has reported a value of 28 661.8 cm^{-1}. The MRDCI estimated ω_e agrees well with the experimental value of 338.6 cm^{-1}. The experimental Si−Te bond length in the $A^1\Pi$ state of SiTe is not yet known, while the present calculations predict $r_e = 2.45$ Å for the state. The potential energy curve shows that the $A^1\Pi$ state is strongly bound, and the A−X transition is expected to be quite strong.

The second root of $^1\Sigma^+$ symmetry is denoted as $E^1\Sigma^+$, and the E−X transition is experimentally observed like other members of silicon chalcogenides. In the UV absorption band of SiTe,[4] the $E^1\Sigma^+$-$X^1\Sigma^+$ system has been located at 33 991 cm^{-1}. The calculated transition energy of this state at equilibrium is reported to be 32 902 cm^{-1} which is, therefore, underestimated by about 1000 cm^{-1}. But there is an excellent agreement between the computed and observed ω_e of the $E^1\Sigma^+$ state of SiTe (see Table 1). Although the experimental bond length of SiTe in the $E^1\Sigma^+$ state is not known, the predicted value is about 2.70 Å. The $E^1\Sigma^+$ state dissociates into the ground state limit with an estimated dissociation energy of only 0.57 eV. In the longer bond length region, the potential energy curve of the $E^1\Sigma^+$ state shows a hump which occurs due to an avoided crossing with the higher root of the same symmetry. At equilibrium, the $E^1\Sigma^+$ state is characterized by more than one configuration. The largest contribution comes from the $\pi^3\pi^*$ (c^2=0.46) configuration. Since the equilibrium bond length of $E^1\Sigma^+$ is 0.41 Å longer than the ground-state bond, the E−X transition is expected to have poor Franck−Condon factors.

Two weakly bound quintets, $^5\Sigma^+$ and $^5\Pi$, dissociate into the ground-state dissociation limit with dissociation energies of 0.56 and 0.44 eV, respectively. Of all the excited states of SiTe, the $^5\Sigma^+$ state has the longest equilibrium bond length. The computed transition energies of $^5\Sigma^+$ and $^5\Pi$ at equilibrium are 32 991 and 33 953 cm^{-1}, respectively. The $^5\Sigma^+$ and $^5\Pi$ states are characterized by $\sigma^2\pi^2\pi^{*2}$ and $\sigma\pi^3\pi^{*2}$ configurations, respectively. Some other higher excited configurations also contribute to these states considerably. The potential energy curve of the $2^3\Pi$ state shows a shallow minimum at $r_e = 2.89$ Å. A very small barrier (∼750 cm^{-1}) appears in the potential energy curve due to an avoided crossing with the higher root of $^3\Pi$.

B. $SiTe^+$. Spectroscopic constants of $SiTe^+$ obtained from the MRDCI calculations at the same level as those of the neutral species are given in Table 2. The equilibrium bond length of the ground state ($X^2\Pi$) of $SiTe^+$ is 2.45 Å with a vibrational frequency of 384 cm^{-1}. The state dissociates into the lowest asymptote with a dissociation energy of 3.66 eV. Potential energy curves of 14 low-lying Λ-S states of $SiTe^+$ are shown in Figure 2. Although no photoelectron spectroscopic study of SiTe has been reported so far, a comparative study with the lighter isovalent species may be useful to check the reliability of the results of $SiTe^+$. The $X^2\Pi$ state of $SiTe^+$ is characterized dominantly by $\sigma^2\pi^3$. Near the potential minimum, the σ MO is a bonding combination of s and p_z AOs of both Si and Te atoms. The π MO is also bonding comprising the p_x AOs.

TABLE 2: Spectroscopic Constants of Low-Lying Λ-S States of $SiTe^+$

state	T_e/cm^{-1}	r_e/Å	ω_e/cm^{-1}
$X^2\Pi$	0	2.45	384
$A^2\Sigma^+$	2558	2.29	449
$^4\Pi$	12 190	2.84	237
$^4\Sigma^+$	15 275	2.53	292
$2^2\Pi$	17 445	2.82	246
$^4\Delta$	18 942	2.62	250
$^4\Sigma^-$	20 784	2.72	199
$B^2\Sigma^+$	22 428	2.51	288
$^2\Sigma^-$	23 487	2.74	187
$^2\Delta$	23 695	2.79	178
$2^4\Sigma^-$	24 654	3.22	199
$2^2\Delta$	27 141	2.69	239
$2\ ^2\Sigma^-$	28 904	2.77	196

The first excited state of $SiTe^+$ is $A\ ^2\Sigma^+$, analogous to that of the other lighter ions.[31−33] The computed $A\ ^2\Sigma^+$-$X^2\Pi$ energy separation is 2558 cm^{-1}, which is larger than in the lighter ions, as expected. The Si−Te bond in the $A\ ^2\Sigma^+$ state is shorter than the ground-state bond by about 0.16 Å, and the computed ω_e value of this state is 449 cm^{-1}. The $A\ ^2\Sigma^+$ state is strongly bound with a dissociation energy of 3.34 eV which is comparable with that of $SiSe^+$. As expected the $\sigma\pi^4$ configuration dominates in this state.

The $2^2\Pi$ state, which is the next higher root of the ground-state symmetry, is sandwiched between two pairs of quartet states. It lies about 17 445 cm^{-1} above the ground state. The potential minimum of the $2^2\Pi$ state is located at 2.82 Å, which is much longer than the ground-state bond length. Two quartets, namely $^4\Pi$ and $^4\Sigma^+$, are placed below the $2^2\Pi$ state, while another two, $^4\Delta$ and $^4\Sigma^-$, lie above. The energy ordering of these states is the same as that of the isovalent $SiSe^+$ ion. The $^4\Pi$ state has a transition energy of 12 190 cm^{-1} with $r_e = 2.84$ Å and $\omega_e = 237$ cm^{-1}. It is strongly bound with a dissociation energy of 2.15 eV. The $^4\Sigma^+$ state has a much shorter bond length (r_e=2.53 Å), and the vibrational frequency is nearly 300 cm^{-1}. The computed transition energies of the $^4\Delta$ and $^4\Sigma^-$ states of $SiTe^+$ are 18 942 and 20 784 cm^{-1}, respectively. All four quartets are spectroscopically significant because their spin components interact strongly with those of the low-lying doublets.

The excited $^2\Sigma^+$ state of $SiTe^+$ looks very similar to the $B^2\Sigma^+$ state of the lighter ions. So, we have also designated the state as $B^2\Sigma^+$. The potential energy curve of $B^2\Sigma^+$ is very smooth and dissociates into a higher asymptote. The transition energy of the state at equilibrium is calculated to be 22 428 cm^{-1}, while the corresponding r_e and ω_e values are 2.508 Å and 288 cm^{-1}, respectively. The dominant configuration that describes the $B^2\Sigma^+$ state is $\sigma\pi^3\pi^*$ (c^2=0.73). The $B^2\Sigma^+$ state is, however, strongly bound with a dissociation energy of about 2.07 eV. Although they have not yet been experimentally observed, the $B^2\Sigma^+$-$X^2\Pi$ and $B^2\Sigma^+$-$A^2\Sigma^+$ transitions are likely to take place in the range 20 000−23 000 cm^{-1}. The nearly degenerate states such as $^2\Sigma^-$ and $^2\Delta$ are located next to $B^2\Sigma^+$. Not only do the potential energy curves of these states look alike, but their spectroscopic constants are also comparable in magnitude (Table 2). The computed transition energies of these

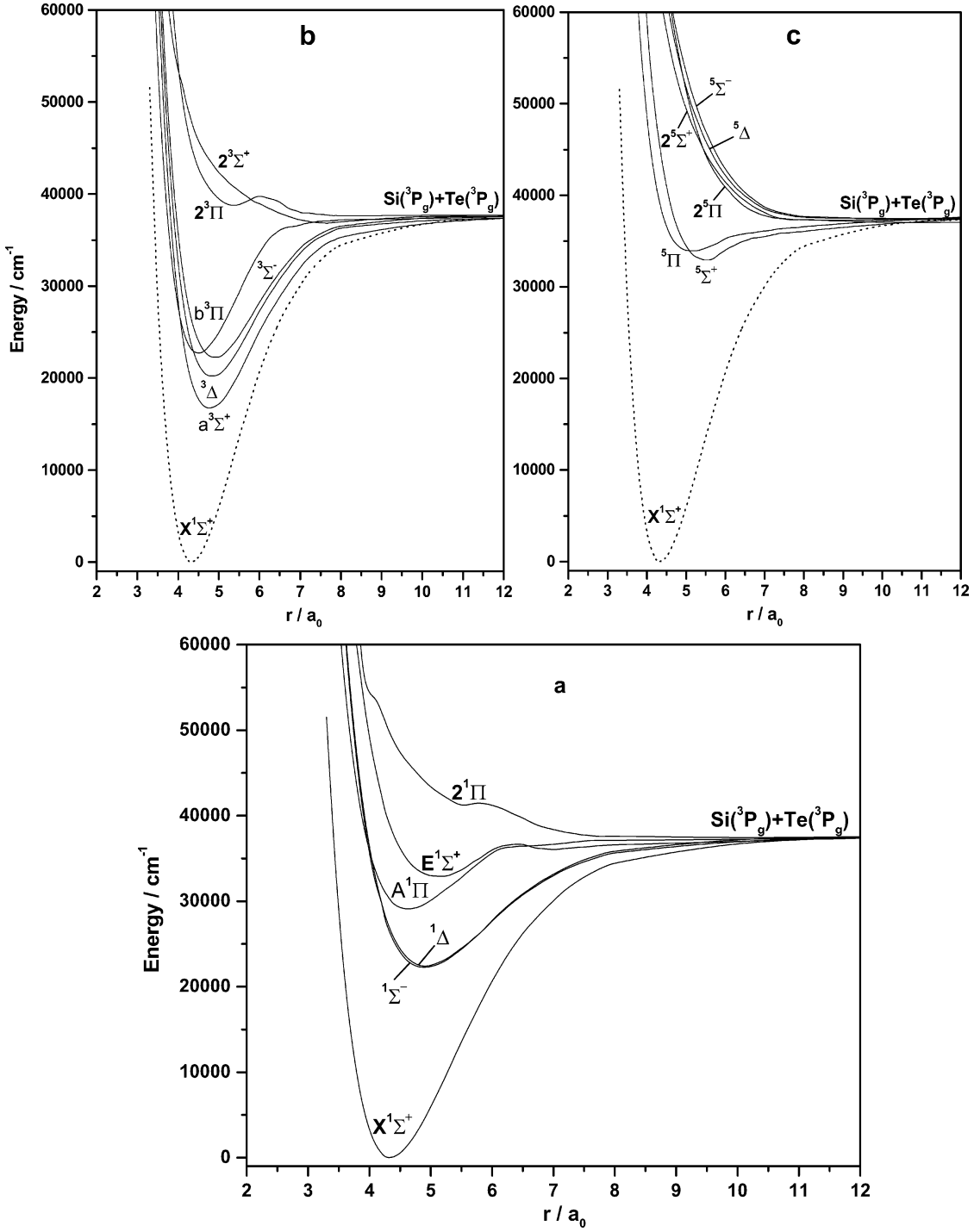

Figure 1. Computed potential energy curves of low-lying Λ-S states of SiTe for (a) singlet, (b) triplet, and (c) quintet spin multiplicities.

states at equilibrium are around 23 500 cm^{-1}. Both $^2\Sigma^-$ and $^2\Delta$ states are described by the same set of configurations dominated by the $\sigma \rightarrow \pi^*$ excitation, and they dissociate into the lowest limit. The second root of the $^4\Sigma^-$ symmetry has a potential minimum at a longer bond length of 3.22 Å. The vibrational frequency of the $2^4\Sigma^-$ state is comparable with that of its lower root. The excited $2^2\Delta$ state, which dissociates into the higher asymptote, has a deep potential well (Figure 2). The computed D_e of the state is about 1.49 eV, and the state lies 27 141 cm^{-1} above the ground state. The bond length of the $2^2\Delta$ state at equilibrium is 2.69 Å with a vibrational frequency of 239 cm^{-1}. Both the $^2\Delta$ and $2^2\Delta$ states are characterized by the same set of configurations. Another state of the $2^2\Sigma^-$ symmetry appears from the same $\sigma\pi^3\pi^*$ configuration as that of either $^2\Delta$ or $2^2\Delta$ state. There is a small barrier at around 3 Å in the potential energy curve of $2^2\Sigma^-$ which is due to an avoided crossing with the curve of the higher root. The $2^2\Sigma^-$ state, however, dissociates into the lowest asymptote through this barrier.

Potential Energy Curves and Spectroscopic Constants of Ω States. A. SiTe. As a result of the spin−orbit coupling, the ^{3}P+^{3}P dissociation limit splits into nine asymptotes which correlate with 50 Ω states. In our spin−orbit calculations, all these states are included. The lowest three asymptotes are separated from others by more than 4500 cm^{-1}. The spin−orbit splittings among the components of $^3P_{0,1,2}$ of Te are large, hence its effects on its spectral properties of SiTe are also correspondingly large. Potential energy curves of 0^+, 0^-, 1, and 3, and 2 states of SiTe are shown in Figure 3a−d.

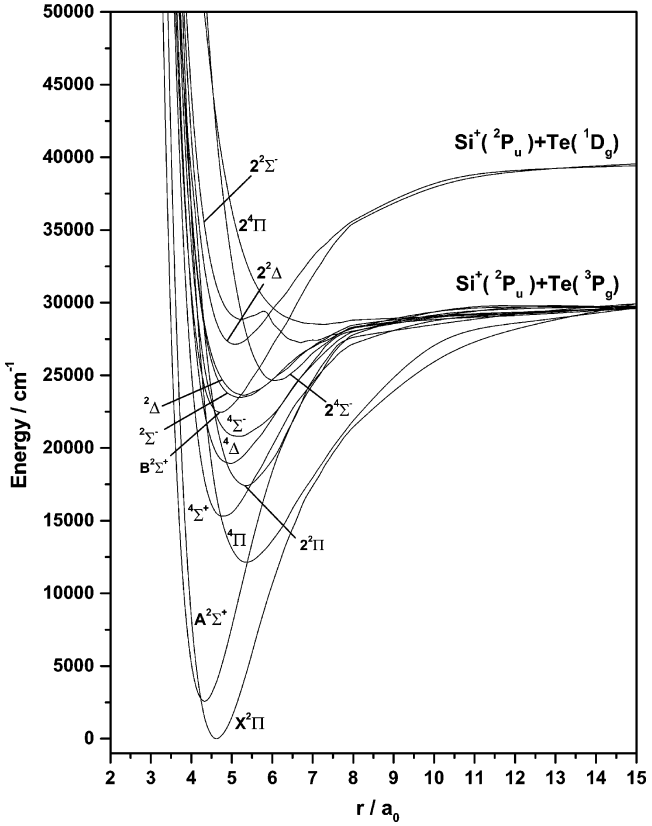

Figure 2. Computed potential energy curves of low-lying Λ-S states of $SiTe^+$.

TABLE 3: Spectroscopic Constants of Ω States of SiTe

state	T_e/cm^{-1}	r_e/Å	ω_e/cm^{-1}	composition at r_e (%)
$X^1\Sigma^+_{0+}$	0	2.30	480	$X^1\Sigma^+$(99)
$a^3\Sigma^+_1$	16 112	2.53	341	$a^3\Sigma^+$(90), $^3\Sigma^-$(8)
$a^3\Sigma^+_{0-}$	16 415	2.53	336	$a^3\Sigma^+$(94), $b^3\Pi$(3), $^1\Sigma^-$(2)
$^3\Delta_3$	18 933	2.57	326	$^3\Delta$(99)
$^3\Delta_2$	19 184	2.56	312	$^3\Delta$(79), $^1\Delta$(19), $b^3\Pi$(2)
$^3\Delta_1$	20 625	2.51	304	$^3\Delta$(67), $b^3\Pi$(27), $^3\Sigma^-$(3), $A^1\Pi$(2)
0^+(II)	21 183	2.47	289	$b^3\Pi$(54), $^3\Sigma^-$(45)
0^-(II)	21 448	2.48	294	$^1\Sigma^-$(50), $b^3\Pi$(49)
1(III)	22 308	2.56	306	$^3\Sigma^-$(70), $b^3\Pi$(12), $^3\Delta$(10), $a^3\Sigma^+$(6)
2(II)	22 359	2.48	313	$b^3\Pi$(53), $^1\Delta$(43), $^3\Delta$(3)
0^+(III)	24 056	2.50	395	$^3\Sigma^-$(53.0), $b^3\Pi$(43.0)
0^-(III)	24 304	2.49	394	$^1\Sigma^-$(47), $b^3\Pi$(46), a $^3\Sigma^+$(6)
1(IV)	24 710	2.48	398	$b^3\Pi$(53), $^3\Sigma^-$(25), $^3\Delta$(15), $a^3\Sigma^+$(5)
2(III)	25 684	2.50	383	$b^3\Pi$(43), $^1\Delta$(39), $^3\Delta$(17)
$A^1\Pi_1$	29 611	2.46	332	$A^1\Pi$(92), $^3\Sigma^-$(3), $^3\Delta$(2)
0^+(IV)	31 637	2.88	235	$^5\Sigma^+$(68), $^5\Pi$(27), 2 $^3\Sigma^-$(2)
2(IV)	31 839	2.83	236	$^5\Sigma^+$(55), $^5\Pi$(36), $b^3\Pi$(4), $4^3\Pi$(3)
$^5\Pi_3$	31 962	2.76	186	$^5\Pi$(96)
1(VI)	32 311	2.73	286	$^5\Sigma^+$(52), $^5\Pi$(29), $A^1\Pi$(13), $b^3\Pi$(2)
$E^1\Sigma^+_{0+}$	33 021	2.72	264	$E^1\Sigma^+$(90), $3^3\Pi$(4), $b^3\Pi$(4)
2(V)	34 068	2.85	236	$^5\Pi$(51), $^5\Sigma^+$(38), $3^3\Pi$(3), $4^3\Pi$(2)
$^5\Pi_1$(I)	34 544	2.79	195	$^5\Pi$(72), $^5\Sigma^+$(12), $3^3\Pi$(5), $2^3\Sigma^+$(6)
0^-(IV)	34 600	2.77	162	$^5\Pi$(78), $2^3\Sigma^+$(10), $3^3\Pi$(8)
0^+(VI)	36 260	2.78	221	$^5\Pi$(55), $^5\Sigma^+$(31), $3^3\Pi$(6), $2^3\Pi$(5)
1(VIII)	36 349	2.82	175	$^5\Pi$(64), $^5\Sigma^+$(20), 2 $^3\Sigma^+$(11)

The computed spectroscopic constants of the low-lying Ω states of SiTe are tabulated in Table 3. There is no nearby 0^+ component to perturb the ground-state component, $X^1\Sigma^+_{0+}$, hence its spectroscopic constants remain almost unchanged. Five excited 0^+ states are shown in Figure 3a. The present calculations predict that b $^3\Pi_{0^+}$ and $^3\Sigma^-_{0^+}$ components mix up strongly so that both 0^+(II) and 0^+(III) states consist of $b^3\Pi$ and $^3\Sigma^-$ almost equally. As a result, spectroscopic parameters of 0^+(II) and 0^+(III) are quite different from those of either $b^3\Pi$ or $^3\Sigma^-$. At equilibrium, the energy separation between 0^+(II) and 0^+(III) is about 3000 cm^{-1}. The 0^+(IV) component is dominated by $^5\Sigma^+$ in the Franck−Condon region. The fifth 0^+ is designated as $E^1\Sigma^-_{0+}$ with an estimated transition energy of 33 021 cm^{-1} at r_e. In the equilibrium bond length region, it is mainly composed of the $E^1\Sigma^+$ state. A shallow potential minimum in the curve of 0^+(VI) is located around the energy of 36 260 cm^{-1}. The mixing between $^5\Pi_{0^+}$ and $^5\Sigma^+_{0^+}$ components is predicted to be strong.

The two spin−orbit components of $a^3\Sigma^+$ are separated only by about 300 cm^{-1}. The r_e and ω_e values remain unchanged for $a^3\Sigma^+_1$ and $a^3\Sigma^-_{0^+}$ component. Three spin components of the $^3\Delta$ state split in the inverted order. The largest spin−orbit splitting in $^3\Delta$ is about 1700 cm^{-1}. The $^3\Delta_2$ component is strongly coupled with $^1\Delta_2$, while $^3\Delta_3$ remains unaffected as there are no nearby components with $\Omega = 3$. The $^3\Delta_1$ component is mixed up strongly with $b^3\Pi_1$ for which the bond is shortened by about 0.05 Å. The computed adiabatic transition energy of $^3\Delta_1$ is around 20 625 cm^{-1}. The 0^- components of $^1\Sigma^-$ and $b^3\Pi$ interact almost equally, and the potential minima of 0^-(II) and 0^-(III) are separated by 2856 cm^{-1}. Due to the strong coupling, the equilibrium vibrational frequency of 0^-(III) is larger than that of 0^-(II) at least by 100 cm^{-1}. However, these 0^- components are not so important from the spectroscopic point of view as no transition is expected to take place.

The sharp potential minima of the 1(III) and 1(IV) states of SiTe appear due to the interaction between $^3\Sigma^-_1$ and $b^3\Pi_1$. The 1(III) state is dominated by $^3\Sigma^-$, while $b^3\Pi_1$ is the leading contributor in 1(IV). Other components such as $^3\Delta_1$ and $a^3\Sigma^+_1$ are also present to some extent. The computed transition energies of 1(III) and 1(IV) at equilibrium are 22 308 and 24 710 cm^{-1}, respectively. The 1(IV) state has a shorter bond length than 1(III) because of the larger participation of the $b^3\Pi$ state. The adiabatic potential energy curves of 2(II) and 2(III) are found to be quite smooth (Figure 3d). A strong coupling between $b^3\Pi_2$ and $^1\Delta_2$ components is shown in the composition of 2(II) and 2(III) (Table 3). The energy separation between 2(II) and 2(III) is estimated to be 3325 cm^{-1}. In the Franck−Condon region, the $A^1\Pi_1$ component is relatively pure with more than 90% contribution from $A^1\Pi$. The potential minimum of this component is located around 29 600 cm^{-1} with $r_e = 2.46$ Å. Spectroscopic constants of 2(IV) and 2(V) estimated from their adiabatic curves are also given in Table 3. The remaining states are mostly dominated by the components of excited quintets.

B. $SiTe^+$. Six asymptotes of $SiTe^+$ arising out of $Si^+(^2P)$+Te(^3P) split within 5038 cm^{-1} of energy due to the spin−orbit coupling. The lowest two dissociation limits, $Si^+(^2P_{1/2})$+Te($^3P_2$) and $Si^+(^2P_{3/2})$+Te($^3P_2$), are located 4400 cm^{-1} below a set of four other limits. The ground state of $SiTe^+$ is $X_1{}^2\Pi_{3/2}$ with $r_e = 2.45$ Å and $\omega_e = 380$ cm^{-1} which are almost the same as those of $X^2\Pi$. However, the $X_2{}^2\Pi_{1/2}$ component has a strong spin−orbit mixing mainly with the $A^2\Sigma^+_{1/2}$ component. Table 4 shows the spectroscopic constants and compositions of Ω states of $SiTe^+$ at the corresponding r_e. The computed r_e and ω_es of the two components of $X^2\Pi$ differ largely due to the strong spin−orbit coupling. The zero-field splitting of the ground state of $SiTe^+$ is 1880 cm^{-1}. The equilibrium bond length of $A^2\Sigma^+_{1.2}$, which is composed of 60% $A^2\Sigma^+$ and 39% $X^2\Pi$, is elongated by 0.07 Å, while its ω_e value is increased by 24 cm^{-1}. The potential energy curves of all low-lying spin−orbit states of 1/2, 3/2, 5/2, and 7/2 symmetries of $SiTe^+$ are shown in Figure 4a,b. Four spin components of $^4\Pi$ split within 560 cm^{-1} of energy. The spectroscopic constants estimated from the adiabatic curves are given in Table 4. The $^4\Sigma^+_{3/2}$ and $^4\Sigma^+_{1/2}$ components are separated by 853 cm^{-1}. The mixing of these

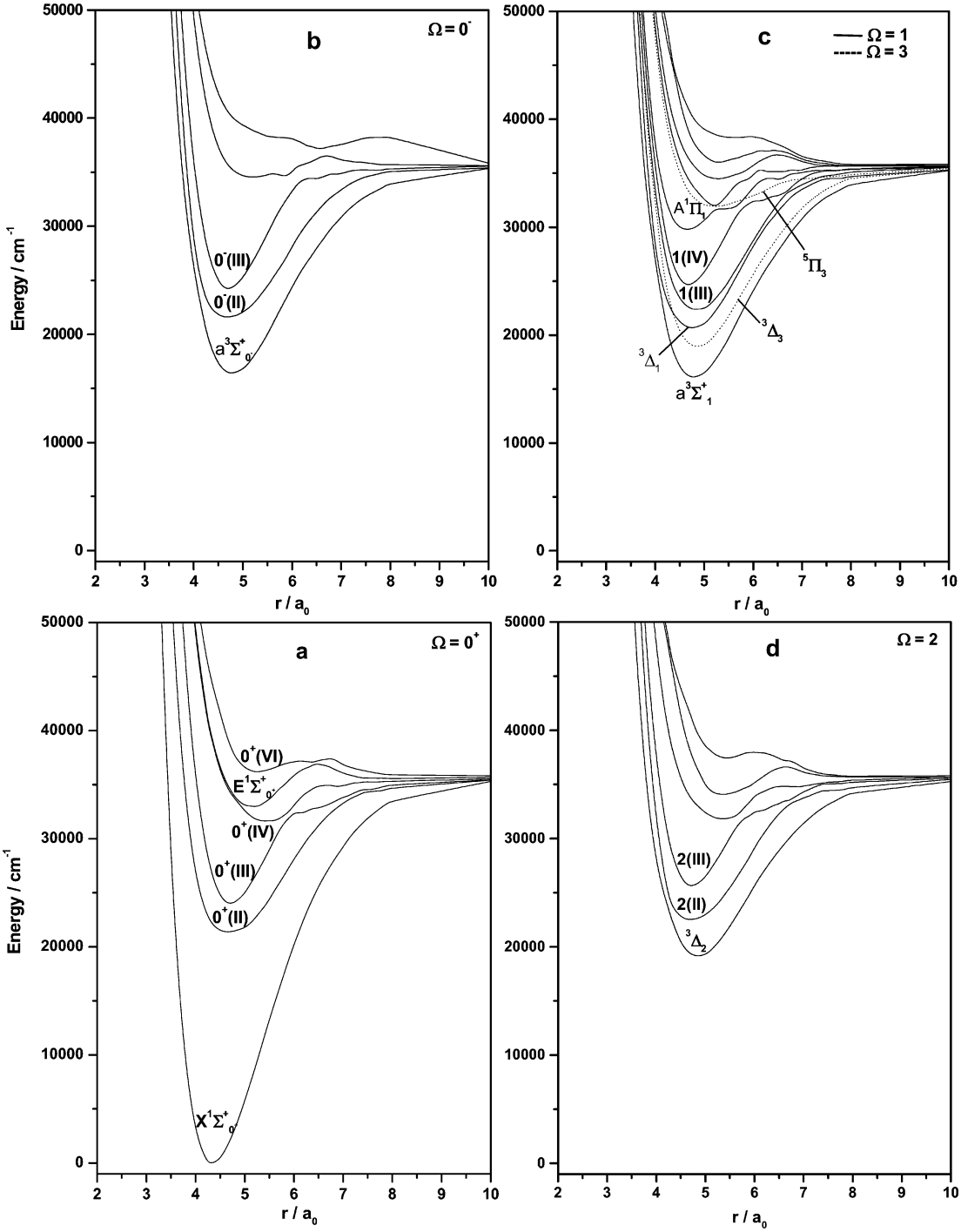

Figure 3. Computed potential energy curves of low-lying Ω states of SiTe for (a) $\Omega = 0^+$, (b) $\Omega = 0^-$, (c) $\Omega = 1,3$, and (d) $\Omega = 2$.

two components with the components of $2^2\Pi$ is found to be significant. The 7/2, 5/2, 3/2, and 1/2 components of $^4\Delta$ split in the inverted order. The two spin components of $2^2\Pi$ lie close to each other. However, their r_e and ω_e values differ considerably due to avoided crossings. The computed energy separation between the two components of $^4\Sigma^+$ is about 325 cm^{-1}. The extent of the spin−orbit coupling is shown in Table 4. The $B^2\Sigma^+_{1/2}$ component is the ninth root of $\Omega = 1/2$ symmetry. Its transition energy and other spectroscopic constants change because of several avoided curve crossings.

Transition Dipole Moments and Radiative Lifetimes of Excited States. A. SiTe. The transition dipole moment functions of five transitions involving Λ-S states of SiTe are shown in Figure 5. The transition moment curve for the $E^1\Sigma^+ - X^1\Sigma^+$ transition has a sharp peak in the Franck−Condon region. Around the equilibrium bond length, the computed transition moment values are more than 1.3 ea_0, which indicates that the E−X transition is quite strong. Transition moments of other transitions are at least 5 times smaller. The computed radiative lifetimes for these five transitions are tabulated in Table 5. The partial lifetime for the $A^1\Pi - X^1\Sigma^+$ transition is predicted to be at least 10 times shorter than that for $E^1\Sigma^+ - X^1\Sigma^+$. Although transition moments for E−X are larger than those for A−X, the Franck−Condon overlap factor is small due to the larger equilibrium bond length of the upper state. Two other transitions from $A^1\Pi$ such as $A^1\Pi - {}^1\Sigma^-$ and $A^1\Pi - {}^1\Delta$ are not as strong as either E−X or A−X. The partial lifetimes for these two transitions are of the order of tens of μs. The $b^3\Pi - a^3\Sigma^+$

TABLE 4: Spectroscopic Constants of Ω States of $SiTe^+$

state	T_e/cm^{-1}	r_e/Å	ω_e/cm^{-1}	composition at r_e (%)
$X_1{}^2\Pi_{3/2}$	0	2.45	380	$X^2\Pi$(99)
$X_2{}^2\Pi_{1/2}$	1880	2.39	348	$X^2\Pi$(71), $A\ ^2\Sigma^+$(28)
$A^2\Sigma^+_{1/2}$	5860	2.36	473	$A\ ^2\Sigma^+$(60), $X^2\Pi$(39)
$^4\Pi_{1/2}$	13 162	2.82	219	$^4\Pi$(87), $^4\Sigma^+$(6), $A\ ^2\Sigma^+$(3)
$^4\Pi_{3/2}$	13 374	2.84	216	$^4\Pi$(91), $^4\Delta$(4)
$^4\Pi_{5/2}$	13 567	2.84	238	$^4\Pi$(94), $^4\Delta$(4)
$^4\Pi_{1/2}$	13 722	2.75	336	$^4\Pi$(91), $^4\Sigma^+$(2), $X^2\Pi$(2)
$^4\Sigma^+_{3/2}$	15 789	2.66	317	$^4\Sigma^+$(71), $2^2\Pi$(15), $^4\Sigma^-$(10)
$^4\Sigma^+_{1/2}$	16 642	2.64	281	$^4\Sigma^+$(62), $2^2\Pi$(22), $^4\Pi$(10), $^2\Sigma^-$(4)
$^4\Delta_{5/2}$	18 527	2.67	222	$^4\Delta$(90)
$^4\Delta_{7/2}$	19 410	2.70	211	$^4\Delta$(96)
$2^2\Pi_{1/2}$	19 566	2.73	262	$2^2\Pi$(54), $^4\Pi$(6), $^4\Sigma^-$(3), $B\ ^2\Sigma^+$(2),
$2^2\Pi_{3/2}$	19 639	2.83	178	$2^2\Pi$(50), $^4\Sigma^-$(16), $^4\Sigma^+$(14), $^2\Delta$(8), $^4\Delta$(4), $^4\Pi$(3)
$^4\Delta_{3/2}$	21 209	2.69	293	$^4\Delta$(60), $2^2\Pi$(33), $^4\Sigma^+$(3)
$^4\Delta_{1/2}$	22 268	2.63	238	$^4\Delta$(89), $^4\Sigma^-$(7)
$^4\Sigma^-_{1/2}$	22 835	2.66	262	$^4\Sigma^-$(69), $B\ ^2\Sigma^+$(10), $^4\Delta$(8), $^4\Pi$(6), $2^2\Pi$(3), $^4\Sigma^+$(2)
$^4\Sigma^-_{3/2}$	23 160	2.70	231	$^4\Sigma^-$(76), $^4\Sigma^+$(16), $4^2\Pi$(6)
3/2(VII)	23 673	2.79	224	$3^2\Pi$(42), $^4\Delta$(29), $^2\Delta$(18), $2^2\Delta$(9)
$B^2\Sigma^+_{1/2}$	24 571	2.64	203	$B^2\Sigma^+$(65), $^4\Sigma^-$(13), $^2\Sigma^-$(10), $2^2\Pi$(5)
$3^2\Pi_{1/2}$	25 579	2.80	182	$3^2\Pi$(85), $^4\Delta$(15)

transition has a partial lifetime of the order of hundreds of μs. Total radiative lifetimes of $E^1\Sigma^+$, $A^1\Pi$, and $b^3\Pi$ at $v' = 0$ are 6.6, 0.63, and 124 μs, respectively.

Partial and total lifetimes of some Ω states of SiTe at the lowest vibrational level are also computed. As the spin−orbit mixing is large, Ω-Ω transition probabilities are important to study. Eight transitions from the excited 0^+ and 1 components to the ground-state component, $X^1\Sigma^+_{0^+}$, have partial radiative lifetimes in the range of 1−100 μs. The lifetime of $E^1\Sigma^+_{0^+}$ at $v' = 0$ is predicted to be 13.8 μs, while that of $A^1\Pi_1$ is less than a microsecond. The spin-forbidden transition such as $a^3\Sigma^+_1$-$X^1\Sigma^+_{0^+}$ is weak with a lifetime of 775 μs.

B. $SiTe^+$. Like the neutral species, transition moments of several low-lying transitions of $SiTe^+$ are calculated using the MRDCI wave functions. Table 6 shows the partial and total radiative lifetimes of the excited Λ-S and Ω states of $SiTe^+$ at the lowest vibrational level. Two symmetry-allowed transitions from $B^2\Sigma^+$ reported here are $B^2\Sigma^+$-$X^2\Pi$ and $B^2\Sigma^+$-$A^2\Sigma^+$. The former transition is found to be much stronger than the later. Combining the transition probabilities of these two transitions, the total radiative lifetime of $B^2\Sigma^+$ is estimated to be 1.7 μs. The partial lifetime for the $2^2\Pi$-$X^2\Pi$ transition is of the order of milliseconds.

Five transitions from the excited 1/2 and 3/2 states to the ground-state component ($X_1{}^2\Pi_{3/2}$) have been studied here. The X_2-X_1 transition is very weak with a long lifetime of 107.6 ms, as is expected for an electric-dipole forbidden transition. This transition is made allowed by the spin−orbit mixing between $X_2{}^2\Pi_{1/2}$ and $A^2\Sigma^+_{1/2}$ states. In our calculations, we have not included the magnetic dipole operator which will otherwise allow the X_1-X_2 transition to take place even in the absence of spin−orbit coupling. The $A-X_1$ transition is much stronger (τ=191 μs at v'=0). The partial lifetime for the $^4\Pi_{3/2}-X_1{}^2\Pi_{3/2}$ transition is 559 μs, hence it is expected to be weak. Three other transitions such as $^4\Pi_{3/2}-X_1{}^2\Pi_{3/2}$, $^4\Sigma^+_{3/2}-X_1{}^2\Pi_{3/2}$, and 2 $^2\Pi_{3/2}-X_1{}^2\Pi_{3/2}$ are also predicted to be weak.

Dipole Moments and Vertical Ionization Energies.. The computed dipole moments (μ_e) of the ground and eight low-lying Λ-S states of SiTe are reported in Table 7. The ground-state dipole moment of SiTe is only −0.17 D, which shows a weak Si^+ Te^- polarity. Therefore, it is predicted that the SiTe molecule is much less polar than the lighter silicon chalcogenides. All the low-lying states of SiTe except $E^1\Sigma^+$ have the opposite polarity. These excited states arise from either $\sigma\rightarrow\pi^*$ or $\pi\rightarrow\pi^*$ transition which enhance the electron density on Si leading to the opposite sense of the ground-state polarity. The dipole moment (μ_e) of the $b^3\Pi$ state is only 0.04 D, while that of the $E^1\Sigma^+$ state is about −0.27 D. Dipole moments of all low-lying states are found to be smooth functions of the bond distance, and they approach to zero at very large bond distances. Table 7 also displays the computed dipole moments of the ground and some low-lying states of $SiTe^+$ at r_e. In the calculations of the ion, the origin has been taken at the center of mass. Although the dipole moments of the ion are origin dependent, their values may be useful in the microwave spectroscopy.

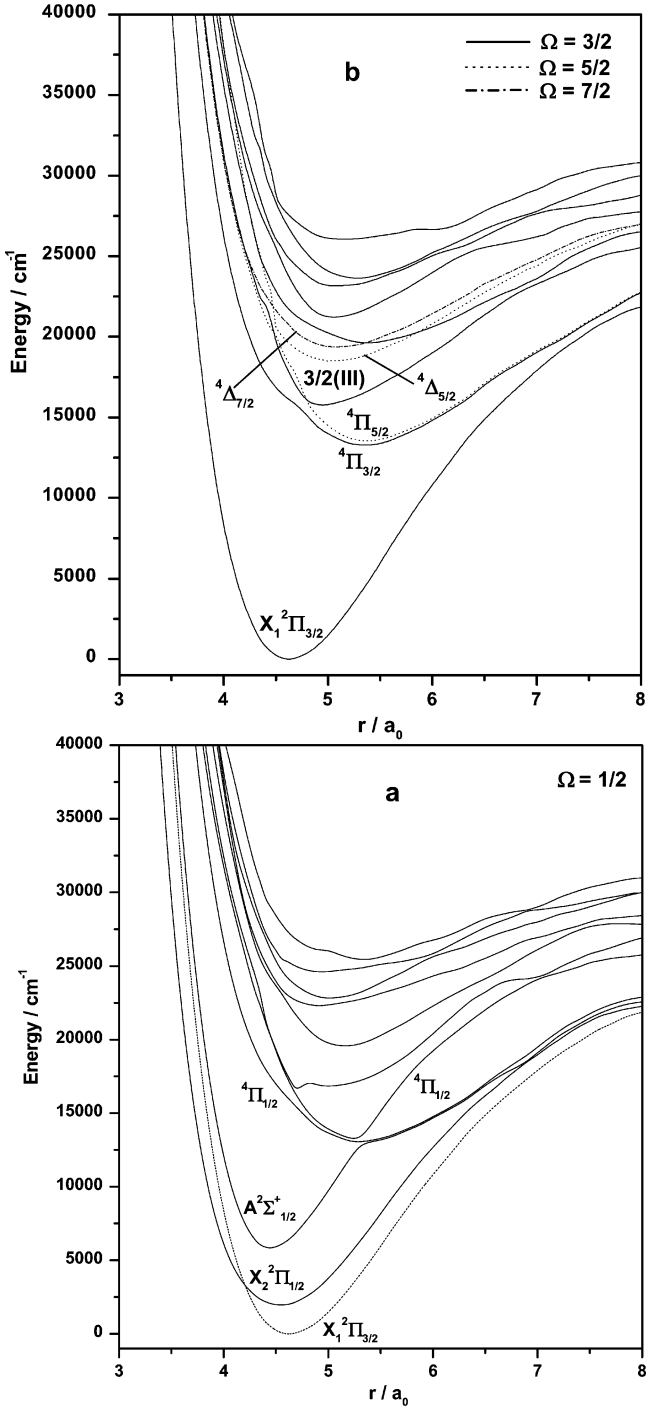

Figure 4. Computed potential energy curves of low-lying Ω states of $SiTe^+$ for (a) Ω = 1/2 and (b) Ω = 3/2, 5/2, 7/2.

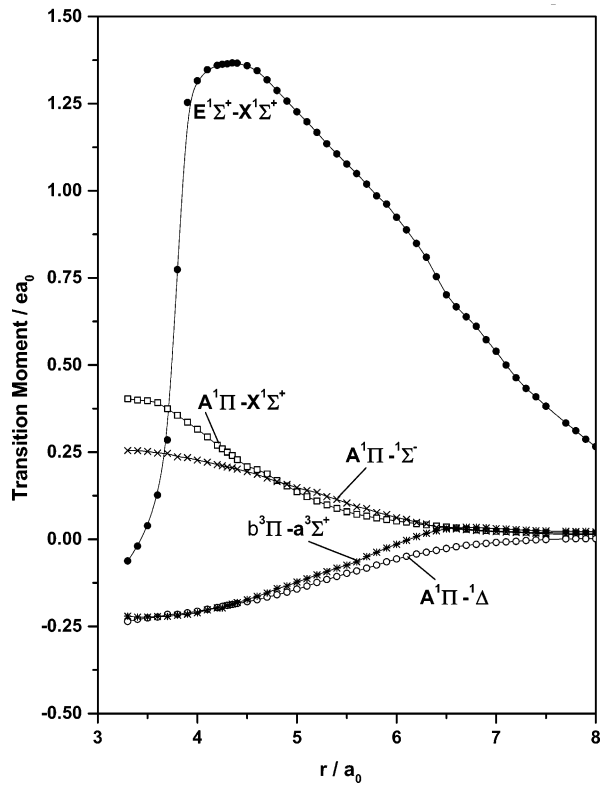

Figure 5. Transition moment curves of five transitions involving Λ-S states of SiTe.

TABLE 5: Radiative Lifetimes (μS) of Some Excited States SiTe at $v' = 0$

transition	partial lifetime of the upper state	total lifetime of the upper state
$E^1\Sigma^+-X^1\Sigma^+$	6.6	$\tau(E\ ^1\Sigma^+) = 6.6$
$A^1\Pi-X^1\Sigma^+$	0.64	$\tau(A^1\Pi) = 0.63$
$A^1\Pi-{}^1\Sigma^-$	65.2	
$A^1\Pi-{}^1\Delta$	85.2	
$b^3\Pi-a^3\Sigma^+$	124.0	$\tau(b^3\Pi) = 124$
$0^+(II)-X^1\Sigma^+_{0+}$	31.5	$\tau(0^+(II)) = 31.5$
$0^+(III)-X^1\Sigma^+_{0+}$	1.6	$\tau(0^+(III)) = 1.6$
$E^1\Sigma^+_{0+}-X^1\Sigma^+_{0+}$	13.8	$\tau(E^1\Sigma^+_{0+}) = 13.8$
$a^3\Sigma^+_1-X^1\Sigma^+_{0+}$	775	$\tau(a^3\Sigma^+_1) = 775$
$^3\Delta_1-X^1\Sigma^+_{0+}$	38.6	$\tau(^3\Delta_1) = 38.6$
$1(III)-X^1\Sigma^+_{0+}$	149	$\tau(1(III)) = 105.5$
$1(III)-a^3\Sigma^+_1$	361	
$1(IV)-X^1\Sigma^+_{0+}$	71	$\tau(1(IV)) = 12$
$1(IV)-a^3\Sigma^+_1$	14.4	
$A^1\Pi_1-X^1\Sigma^+_{0+}$	1.1	$\tau(A^1\Pi_1) = 0.6$
$A^1\Pi_1-a^3\Sigma^+_1$	1.51	

The vertical ionization energies (VIE) of ground-state SiTe to low-lying ionic states have been calculated from the differences in the estimated full-CI energies of the neutral and ionic species at the same level of MRDCI calculations. The basis sets and configuration selection threshold have been kept the same in both sets of calculations. The ground-state bond length of SiTe has been fixed at $r_e = 2.30$ Å which is computed from the MRDCI calculations (Table 1). The energy for the ionization of the ground-state SiTe to the ground state of its ion is 9.21 eV, while ionizations to $A^2\Sigma^+$ and $B^2\Sigma^+$ states of $SiTe^+$ require 9.31 and 12.03 eV of energy, respectively. However, no photoelectron spectrum of SiTe is available for comparison. The VIEs of some other ionic states are listed in Table 7.

TABLE 6: Radiative Lifetime (*s*) of Some Excited States of $SiTe^+$ at $v' = 0$[a]

transition	partial lifetime of the upper state	total lifetime of the upper state
$B^2\Sigma^+-X^2\Pi$	1.70(−6)	$\tau(B^2\Sigma^+) = 1.7(-6)$
$B^2\Sigma^+-A\ ^2\Sigma^+$	2.03(−3)	
$2^2\Pi-X^2\Pi$	6.76(−3)	$\tau(2^2\Pi) = 6.76(-3)$
$X_2{}^2\Pi_{1/2}-X_1{}^2\Pi_{3/2}$	107.6(−3)	$\tau(X_2{}^2\Pi_{1/2}) = 107.6(-3)$
$A^2\Sigma^+_{1/2}-X_1{}^2\Pi_{3/2}$	191.2(−6)	$\tau(A^2\Sigma^+{}_{1/2}) = 191.2(-6)$
$^4\Pi_{3/2}-X_1{}^2\Pi_{3/2}$	559(−6)	$\tau(^4\Pi_{3/2}) = 559(-6)$
$^4\Sigma^+{}_{3/2}-X_1{}^2\Pi_{3/2}$	111.8(−6)	$\tau(^4\Sigma^+{}_{3/2}) = 111.8(-6)$
$2^2\Pi_{3/2}-X_1{}^2\Pi_{3/2}$	5.2(−3)	$\tau(2^2\Pi_{3/2}) = 5.2(-3)$

[a] Values in the parentheses are the powers to the base 10.

TABLE 7: Computed Dipole Moments (μ_e) and Vertical Ionization Energies (VIE) of SiTe[a]

molecule	state	μ_e/D	ion	state	μ_e/D	VIE/eV
SiTe	$X^1\Sigma^+$	−0.17	$SiTe^+$	$X^2\Pi$	3.91	9.21
	$a^3\Sigma^+$	1.38		$A^2\Sigma^+$	3.90	9.31
	$^3\Delta$	0.84		$^4\Pi$	2.99	11.95
	$^3\Sigma^-$	0.49		$^4\Sigma^+$	2.92	11.24
	$^1\Sigma^-$	0.37		$^4\Delta$	3.75	11.82
	$^1\Delta$	0.19		$^4\Sigma^-$	4.93	12.21
	$b^3\Pi$	0.04		$B^2\Sigma^+$		12.03
	$A^1\Pi$	0.28		$^2\Sigma^-$	4.58	12.54
	$E^1\Sigma^+$	−0.27		$^2\Delta$	4.96	12.58

[a] Origin at the center of mass.

IV. Summary

Potential energy curves and spectroscopic properties of the low-lying electronic states of the heaviest silicon chalcogenide, namely SiTe and its monopositive ion, have been explored from the results of the calculations carried out by using the pseudopotential based MRDCI methodology. Unlike the heavier isovalent species, SiTe/$SiTe^+$ have seldom been studied, either experimentally or theoretically. Only the UV absorption studies of the neutral species have been performed in the past. The ground-state bond lengths of SiTe and $SiTe^+$ are 2.30 and 2.45 Å, while their vibrational frequencies are 479 and 384 cm^{-1}, respectively. The computed ground-state dissociation energies of these two species are 4.65 and 3.66 eV, respectively, in the absence of any spin−orbit coupling. With the inclusion of the spin−orbit interaction, the ground-state component of SiTe has a dissociation energy of 4.41 eV, while for the $X_1{}^2\Pi_{3/2}$ component of $SiTe^+$, the dissociation energy is reduced to 3.52 eV. The thermodynamically derived dissociation energy of SiTe agrees well with the computed one. Spectroscopic constants of several low-lying states of SiTe are computed. Two singlets, $A^1\Pi$ and $E^1\Sigma^+$, are experimentally known in the UV absorption spectra of SiTe. The calculated T_e and ω_e of these states match well with the measured values. At least 13 low-lying Λ-S states of $SiTe^+$ are studied here. The first excited state of $SiTe^+$, $A^2\Sigma^+$, lies 2558 cm^{-1} above the ground state, while the transition energy of the next higher root of the same symmetry ($B^2\Sigma^+$) is 22 428 cm^{-1}. The effects of the spin−orbit coupling are large for both SiTe and $SiTe^+$. For the ion, the ground-state spin−orbit splitting is estimated to be 1880 cm^{-1} with $X_1{}^2\Pi_{3/2}$ being the lower component. The adiabatic potential curves of the spin−orbit states are fitted throughout for the estimation of the spectroscopic parameters. Several transitions such as $E^1\Sigma^+_{0+}-X^1\Sigma^+_{0+}$, a $^3\Sigma^+_1-X^1\Sigma^+_{0+}$, $A^1\Pi_1-X^1\Sigma^+_{0+}$, and $A^1\Pi_1-a^3\Sigma^+_1$ of SiTe are studied. Since the $X_2{}^2\Pi_{1/2}-X_1{}^2\Pi_{3/2}$ transition of $SiTe^+$ is weak in intensity, it may not be possible to observe it using current spectroscopic methods. The other transition, $A^2\Sigma^+_{1/2}-X_1{}^2\Pi_{3/2}$ is spectroscopically important and should be observed experimentally. The partial radiative lifetimes for these

transitions are predicted to be 108 ms and 191 μs, respectively. The calculated VIE of the ground-state SiTe to the ground-state $SiTe^+$ is about 9.21 eV. Other VIEs to excited ionic states are also computed.

Acknowledgment. The authors thank Prof. Dr. Robert J. Buenker, Bergische Universität, Wuppertal, Germany for allowing us to use the CI codes.

References and Notes

(1) Barrow, R. F.; Jevons, W. *Proc. R. Soc. Ser.* **1938**, *A169*, 45.
(2) Barrow, R. F. *Proc. Phys. Soc.* **1939**, *51*, 267.
(3) Barrow, R. F.; Jevons, W. *Proc. R. Soc.* **1938**, *A169*, 49.
(4) Vago, E. E.; Barrow, R. F. *Proc. Phys. Soc.* **1946**, *58*, 538.
(5) Exsteen, G.; Drowart, J.; Vander Auwera-Mahieu, A. *J. Phys. Chem.* **1967**, *71*, 4130.
(6) Brebrick, R. F. *J. Chem. Phys.* **1968**, *49*, 2584.
(7) Lakshminarayana, G.; Shetty, B. J. *J. Mol. Spectrosc.* **1993**, *161*, 575.
(8) Cockett, M. C. R.; Dyke, J. M.; Morris, A.; Niavaran, M. H. Z. *J. Chem. Soc., Faraday Trans. 2* **1989**, *85*, 75.
(9) Lebreton, J.; Bosser, G.; Ferran, J.; Marsigny, L. *J. Phys. B* **1975**, *8*, L141.
(10) Bosser, G.; Marsigny, L. *J. Chim. Phys.* **1977**, *74*, 13.
(11) Chattopadhyaya, S.; Das, K. K. *Chem. Phys. Lett.* **2004**, *399*, 140.
(12) Pacios, L. F.; Christiansen, P. A. *J. Chem. Phys.* **1985**, *82*, 2664.
(13) LaJohn, L. A.; Christiansen, P. A.; Ross, R. B.; Atashroo, T.; Ermler, W. C. *J. Chem. Phys.* **1987**, *87*, 2812.
(14) Matos, J. M. O.; Kellö, V.; Ross, B. O.; Sadlej, A. J. *J. Chem. Phys.* **1988**, *89*, 423.
(15) Setzer, K. D.; Fink, E. H.; Alekseyev, A. B.; Liebermann, H.-P.; Buenker, R. J. *J. Mol. Spectrosc.* **2001**, *206*, 181.
(16) Buenker, R. J.; Peyerimhoff, S. D. *Theo. Chim. Acta* **1974**, *35*, 33.
(17) Buenker, R. J.; Peyerimhoff, S. D. *Theo. Chim. Acta* **1975**, *39*, 217.
(18) Buenker, R. J. *Int. J. Quantum Chem.* **1986**, *29*, 435.
(19) Buenker, R. J. In *Proceedings of the Workshop on Quantum Chemistry and Molecular Physics*; Burton, P., Ed.; University Wollongong: Wollongong, Australia, 1980.
(20) Buenker, R. J. In *Studies in Physical and Theoretical Chemistry*; Carbo, R., Ed.; Elsevier: Amsterdam, The Netherlands, 1982; Vol. 21 (Current Aspects of Quantum Chemistry).
(21) Buenker, R. J.; Peyerimhoff, S. D.; Butscher, W. *Mol. Phys.* **1978**, *35*, 771.
(22) Buenker, R. J.; Philips, R. A. *J. Mol. Struct. (THEOCHEM)* **1985**, *123*, 291.
(23) Krebs, S.; Buenker, R. J. *J. Chem. Phys.* **1995**, *103*, 5613.
(24) Alekseyev, A. B.; Buenker, R. J.; Liebermann, H.-P.; Hirsch, G. *J. Chem. Phys.* **1994**, *100*, 2989.
(25) Moore, C. E. *Atomic Energy Levels*; U.S. National Bureau of Standards: Washington, DC, 1971; Vol. I−III.
(26) Huber K. P.; Herzberg, G. In *Molecular Spectra and Molecular Structure*; Van Nostrand Reinhold: Princeton, NJ, 1979; Vol. 4 (Constants of Diatomic Molecules).
(27) Chattopadhyaya, S.; Chattopadhyay, A.; Das, K. K. *J. Phys. Chem.* **2003**, *A107*, 148.
(28) Chattopadhyaya, S.; Chattopadhyay, A.; Das, K. K. *J. Phys. Chem.* **2002**, *A106*, 833.
(29) Chattopadhyaya, S.; Das, K. K. *Chem. Phys. Lett.* **2003**, *382*, 249.
(30) Linton, C. *J. Mol. Spectrosc.* **1980**, *80*, 279.
(31) Chattopadhyaya, S.; Chattopadhyay, A.; Das, K. K. *J. Mol. Struct. (THEOCHEM)* **2003**, *639*, 177.
(32) Chattopadhyaya, S.; Das, K. K. *J. Phys. B: At., Mol. Opt. Phys.* **2004**, *37*, 3355.
(33) Chattopadhyaya, S.; Das, K. K. *Chem. Phys. Lett.* **2004**, *399*, 140.